Development of Amperometric and Microgravimetric Immunosensors and Reversible Immunosensors Using Antigen and Photoisomerizable Antigen Monolayer Electrodes

Ron Blonder, Shlomo Levi, Guoliang Tao, Iddo Ben-Dov, and Itamar Willner*

Contribution from the Institute of Chemistry and The Farkas Center for Light-Induced Processes, The Hebrew University of Jerusalem, Jerusalem 91904, Israel

Received June 16, 1997[⊗]

Abstract: Antigen monolayers assembled onto Au-electrodes or Au-electrodes associated with quartz crystals act as active interfaces for the amperometric or microgravimetric analysis of the complementary antibody and provide the grounds for the development of electrochemical and piezoelectric immunosensors. The antigen monolayer of Nϵ-2,4-dinitrophenyl-L-lysine is assembled on an electrode. The *anti*-dinitrophenyl antibody, *anti*-DNP-Ab, is sensed by the antigen monolayer, and the formation of the antigen−antibody complex at the monolayer interface is probed by the insulation of the electrode toward a redox probe in the electrolyte solution. The formation of the antibody−antigen complex is amplified by the application of the *anti*-antibody or the use of a ferrocene-functionalized redox-enzyme, glucose oxidase, as redox probe. A 3,5-dinitrosalicylic acid antigen monolayer bound to Au-electrodes associated with a quartz crystal is used as active interface for the microgravimetric, quartz-crystal-microbalance analysis of the *anti*-DNP-Ab. Photoisomerizable antigen monolayer electrodes provide the basis for tailoring reversible immunosensors. The dinitrospiropyran monolayer, SP-state, is assembled on Au-electrodes or quartz crystals. The monolayer exhibits reversible photoisomerizable features, and irradiation of the SP-monolayer, $360 < \lambda < 380$ nm, yields the protonated merocyanine monolayer, MRH^+-state. Further irradiation of the MRH^+-monolayer electrode, $\lambda > 495$ nm, restores the SP-monolayer electrode. The SP-monolayer acts as antigen for *anti*-DNP-Ab, whereas the MRH^+-monolayer lacks antigen properties for *anti*-DNP-Ab. This enables the amperometric or piezoelectric transduction of the formation of the antigen−*anti*-DNP-Ab complex at the SP-monolayer interface. By photoisomerization of the monolayer to the MRH^+-state, the Ab is washed-off from the sensing interface. Subsequent light-induced isomerization of the monolayer to the SP-state regenerates the electrochemically or piezoelectrically active sensing interfaces.

Introduction

The high specificity of antibody−antigen interactions and the possibility to elicit antibodies against a variety of nonbiological materials or synthetic fragments of complex biological antigens opens the way to develop a variety of immunosensor devices for clinical diagnosis, environmental pollutants, and food analysis.[1] Radioisotopic labeling of antibodies and antigens was extensively applied in the last three decades in immunoassays.[2] The disadvantages associated with the use of radioactive materials led to the development of other antibody and antigen labels. Enzyme-linked immunosorbant assays (ELISA) were extensively developed as a general immunoassay method, and the enzyme-linked label provides a means to amplify the resulting antigen−antibody (Ab) complex formation.[3] Development of fluorescence,[4] chemiluminescence,[5] or electrode potential changes[6] as a result of the enzyme reactions provide means for the physical or optical transduction of the formation of antigen−antibody complexes.

Electrochemical detection of antibody−antigen interactions was the subject of several research efforts. Capacitance changes at the electrode/electrolyte interface as a result of the formation of antigen−Ab complexes was employed to develop a series of Capacitive Affinity Sensors.[7] Amperometric detection[8] of antigen−Ab complexes was accomplished by the application of redox-modified antigens or antibodies and their competitive association to an electrode interface in the presence of the analyte/substrate (i.e., antigen or Ab, respectively). Enhanced sensitivity in the amperometric detection of antibodies or antigens was achieved by the use of enzyme-linked antibodies or antigens. Antigens or antibodies modified by redox-enzymes enabled the detection of analyte antigens or antibodies, respectively, by their competitive association to electrode surfaces and amperometric transduction of the formation of the antigen−Ab complex at the electrode interface via the enzyme-characteristic bioelectrocatalyzed transformation.[9,10] Indirect electrochemical detection of antibody−antigen complexes was reported using enzyme labels that produce electroactive species which are sensed by the electrode.[11,12] Amperometric or potentiometric

* To whom correspondence should be addressed. Tel.: 972-2-6585272. Fax: 972-2-6527715.

⊗ Abstract published in *Advance ACS Abstracts,* October 1, 1997.

(1) Van Emon, J. P.; Lopez Avila, Y. *Anal. Chem.* **1992**, *64*, 79A.
(2) Garvey, J. S.; Cremer, N. E.; Sussdorf, D. H. *Methods in Immunology*, 3rd ed.; W. A. Benjamin, Inc.: 1977; pp 301−312.
(3) Engrall, E. *Methods in Enzymology*; 1980; Vol. 70, pp 419−439.
(4) Diamandis, E. P.; Christopoulos, T. K. *Anal. Chem.* **1990**, *62*, 1149A.
(5) Hage, D. S.; Kao, P. C. *Anal. Chem.* **1991**, *63*, 586.
(6) Biotieux, J. L.; Thomas, D.; Desment, G. *Anal. Chim. Acta* **1984**, *163*, 309.
(7) Bresler, H. S.; Lenkevich, M. J.; Murdock, J. F.; Newman, A. L.; Roblin, R. O. In *Biosensors Design and Application*; Mathewson, P. R., Finley, J. W., Eds.; ACS Symposium Series, Series 511; American Chemical Society: Washington, DC, 1992; pp 89−104.
(8) *Electrochemical Sensors in Immunological Analysis*; Ngo, T. T., Ed.; Plenum Press: 1987, New York.
(9) Ho, W. O.; Athey, D.; McNeil, C. J. *Biosens. Bioelectron.* **1995**, *10*, 683.
(10) Rishpon, J.; Soussan, L.; Rosen-Margalit, I.; Hadas, E. *Immunoassays* **1992**, *13*, 231.
(11) Wehmeyer, K. R.; Halsall, H. B.; Heineman, W. R.; Volle, C. P.; Chen, C. *Anal. Chem.* **1986**, *58*, 135.
(12) Tsuji, I.; Egushi, H.; Yasukouchi, K.; Unoki, M.; Taniguchi, I. *Biosens. Bioelectron.* **1990**, *5*, 87.

S0002-7863(97)01980-X CCC: $14.00

detection of NADH, phenol, O_2, H_2O_2, or NH_3 generated by the enzymes linked to the antigen or Ab were used to probe antigen−Ab interactions.

Other immunosensor devices are based on the alteration of the physical properties of piezoelectric crystals or the properties of metal surfaces as a result of the formation of antigen−Ab complexes. Microgravimetric analysis of antigens or antibodies by the frequency changes of piezoelectric crystals, i.e., quartz crystals, as a result of mass changes originating from the formation of antigen−Ab complexes on the crystal, provides a sensitive method to develop immunosensors.[13−16] Alteration of the optical properties of thin metal surfaces, i.e., silver or gold, by the formation of antigen−Ab complexes enabled the development of new immunosensor devices. The surface plasmon resonance (SPR) angle at thin metal surfaces is controlled by the dielectric function of the metal surface and film thickness of adsorbate layers. This led to the development of biospecific interaction analyses by SPR-transduction.[17,18]

In a series of recent reports, we addressed the application of functionalized monolayer-electrodes as sensing interfaces for biospecific interactions. Redox-enzyme monolayers and multilayers assembled onto Au-electrodes were applied for the amperometric analysis of various substrates.[19−22] Antigen monolayers assembled onto Au-electrodes were applied for the electrochemical detection of antigen−Ab complex formation at electrode surfaces. In a preliminary report we demonstrated that the insulation of the electrode surface toward a redox probe solubilized in the electrolyte by the formation of the antigen−Ab complex provides a general route for the amperometric transduction of biospecific interactions at the electrode surface.[23] Similarly, functionalized monolayer electrodes associated with quartz crystals were employed for microgravimetric quartz-crystal-microbalance, QCM, analyses of biospecific interactions at the crystal monolayer interface.[24]

The tight antigen−Ab interactions turn the immunosensor devices into single-cycle sensing interfaces. The development of means to recycle immunosensing interfaces could represent a major advance in biosensor technology. The control of biomaterial functions[25,26] and biospecific interactions[27−29] by external light signals was extensively developed by our laboratory, and the advance in this area was recently reviewed.[30,31] Photoregulated binding of a *trans*-azobenzene hapten to the respective antibody[32] and selective association of a dinitrospiropyran with the *anti*-DNP-Ab[33] revealed optically-stimulated association and dissociation of photoizomerizable antigens with their antibodies. It was suggested[23] that reversible photoisomerizable antigens could act as a general method to tailor cyclic, reusable, immunosensor interfaces. In one isomer state of the antigen, the biospecific interactions with the Ab are retained and allow the analysis of the formation of the antigen−Ab complex. In the complementary photoisomer state the antigen-structure is distorted into a configuration that lacks antigen features or affinity, for the Ab. This enables one to wash-off the Ab and then recycle the active antigen layer by a secondary photoisomerization process. In a preliminary note[23] we have demonstrated that a dinitrospiropyran monolayer, assembled onto a Au-surface, allows the cyclic analysis of the dinitrophenyl antibody, DNP-Ab.

Here we present the comprehensive study that describes the methodologies to tailor antigen-monolayer-electrodes for the electrochemical and microgravimetric, quartz-crystal-microbalance, QCM, sensing of antigen−antibody interactions at the electrode surfaces. In addition, we address the novel method to photostimulate the biospecific interactions between an antigen and antibody by the application of a photoisomerizable antigen. We demonstrate the electrochemical and microgravimetric, quartz crystal microbalance, QCM, transduction of the antibody association and dissociation from photoisomerizable antigen-monolayer electrodes and discuss the results in terms of the design of reversible immunosensors.

Experimental Section

Materials. Mercaptobutyl dinitrospiropyran,[34] **1**, and *N*-(2-methylferrocene) caproic acid,[35] **2**, were prepared according to reported methods. Ferrocene-modified GOx, Fc-GOx, was prepared by coupling of *N*-(2-methylferrocene) caproic acid, **2**, to GOx. To a mixture of dry THF (1 mL) that included the ferrocene derivative, **2**, 0.06 g, and *N*-hydroxysuccinimide (NHS), 0.017 g, was added a THF solution (1 mL) that included dicyclohexylcarbodiimide (DCC), 0.031 g. The resulting mixture was stirred for 10 min at 0 °C and filtered. From the *in situ* generated solution of the *N*-hydroxy succinimide active ester of the ferrocene derivative, 400 μL were added to 1.6 mL of distilled water that included $NaHCO_3$, 0.06 g, and GOx (from *Aspergillus niger*, EC 1.1.3.4., Sigma), 100 mg. The resulting mixture was stirred for 24 h at 4 °C. The solution was dialyzed against phosphate buffer, 0.01 M, pH = 7.0, centrifuged, and lyophilized to yield the powder of the ferrocene-modified glucose oxidase, Fc-GOx. The loading of the enzyme by the ferrocene units was determined by using fluorescamine as a probe.[36] *anti*-DNP-Ab is a commercial monoclonal *anti*-dinitrophenyl IgE antibody (Sigma). *anti*−*anti*-DNP-Ab is an IgG *anti*-mouse-IgE (epsilon chain) produced in goat. This antibody is commercially available (Sigma) in a serum solution. To clean the antibody from the other proteins of the serum, we used the ammonium sulfate precipitation method, taking into account the molecular weight of the antibody (150 000 g·mol^{-1} for IgG). In the first state we removed large proteins that may precipitate with low concentration of ammonium

(13) Suleiman, A. A.; Guilbault, G. G. *Analyst* **1994**, *119*, 2279.
(14) Kösslinger, C.; Drost, S.; Aberl, F.; Wolf, H.; Koch, S.; Woias, P. *Biosens. Bioelectron.* **1992**, *7*, 397.
(15) Guilbault, G. G.; Hock, B.; Schmid, R. *Biosens. Bioelectron.* **1992**, *7*, 411.
(16) König, B.; Grätzel M. *Anal. Chem.* **1994**, *66*, 341.
(17) Mrksich, M.; Sigal, G. B.; Whitesides, G. M. *Langmuir* **1995**, *121*, 4383.
(18) Davies, J.; Roberts, C. J.; Dawkes, A. C.; Sefton, J.; Edwards, J. C.; Glasbey, T. O.; Haymes, A. G.; Davies, M. C.; Jackson, D. E.; Lomas, M.; Shakesheff, K. M.; Tendler, S. J. B.; Wilkins, M. J.; Williams, P. M. *Langmuir* **1994**, *10*, 2654.
(19) Katz, E.; Riklin, A.; Willner, I. *J. Electroanal. Chem.* **1993**, *354*, 129.
(20) Willner, I.; Riklin, A.; Shoham, B.; Rivenzon, D.; Katz, E. *Adv. Mater.* **1993**, *5*, 912.
(21) Willner, I.; Katz, E.; Riklin, A.; Kasher, R. *J. Am. Chem. Soc.* **1992**, *114*, 10965.
(22) Willner, I.; Lapidot, N.; Riklin, A.; Kasher, R.; Zahavy, E.; Katz, E. *J. Am. Chem. Soc.* **1994**, *116*, 1428.
(23) Willner, I.; Blonder, R.; Dagan, A. *J. Am. Chem. Soc.* **1994**, *116*, 9365.
(24) Cohen, Y.; Levi, S.; Rubin, S.; Willner, I. *J. Electroanal. Chem.* **1996**, *417*, 65.
(25) Willner, I.; Rubin, S.; Riklin, A. *J. Am. Chem. Soc.* **1991**, *113*, 3321.
(26) Aizawa, M.; Namba, K.; Suzuki, S. *Arch. Biochem. Biophys.* **1977**, *182*, 305.
(27) Willner, I.; Rubin, S.; Wonner, J.; Effenberger, F.; Bäuerle, P. *J. Am. Chem. Soc.* **1992**, *114*, 3150.
(28) Willner, I.; Rubin, S.; Cohen, Y. *J. Am. Chem. Soc.* **1993**, *115*, 4937.
(29) Willner, I.; Lion-Dagan, M.; Marx-Tibbon, S.; Katz, E. *J. Am. Chem. Soc.* **1995**, *117*, 6581.
(30) Willner, I.; Willner, B. In *Bioorganic Photochemistry: Biological Application of Photochemical Switches*; Morrison, H., Ed.; Wiley: New York, 1993; Vol. 2, pp 1−110.
(31) Willner, I.; Rubin, S. *Angew. Chem., Int. Ed. Engl.* **1996**, *35*, 367.
(32) Harada, M.; Sisido, M.; Hirose, J.; Nakanishi, M. *FEBS Lett.* **1991**, *286*, 6.
(33) Willner, I.; Blonder, R.; Dagan, A. *J. Am. Chem. Soc.* **1994**, *116*, 3121.
(34) Willner, I.; Doron, A.; Katz, E.; Levi, S.; Frank, A. J. *Langmuir* **1996**, *12*, 946.
(35) Shoham, B.; Migron, Y.; Riklin, A.; Willner, I.; Tartakovsky, B. *Biosens. Bioelectron.* **1995**, *10*, 341.
(36) Stein, S.; Bohlen, P.; Dairman, W. *Science* **1972**, *178*, 871.

sulfate. To 1 mL of the antibody solution that was stirred gently, we added slowly 0.25 mL saturated ammonium sulfate that had been adjusted to neutral pH with HCl. After all the ammonium sulfate had been added, the solution was left at 4 °C overnight. The solution was centrifuged at 3000*g* for 30 min, and the supernatant was removed and transferred into a clean tube. In the second state, we precipitated the antibody. While the antibody solution was gently stirred, we slowly added enough saturated ammonium sulfate to bring the final concentration to 50% (v/v) saturation (0.75 mL). The solution was left at 4 °C overnight. The solution was centrifuged at 3000*g* for 30 min. The supernatant was carefully removed and discarded. The precipitation was resuspended in 0.5 PBS buffer. The antibody solution was transferred to a dialysis tube and was dialyzed versus PBS at 4 °C overnight.

All other materials were of commercial source (Aldrich or Sigma).

Electrode Characterization and Electrochemical Set-Up. Gold electrodes (0.5 mm diameter of geometrical area of ca. 0.2 cm^2) were used for all modifications and measurements. A cyclic voltammogram of each electrode was recorded in 0.5 M H_2SO_4 and was used to determine the purity of the electrode surface prior to modification. The real electrode surface area and the roughness coefficient (ca. 2.2) were estimated from the same cyclic voltammogram by integrating the cathodic peak for the electrochemical reduction of the oxide layer on the electrode surface. Electrochemical measurements were performed using a potentiostat (EG&G VersaStat) connected to a personal computer (EG&G research electrochemistry software model 270/250). All measurements were carried out in a three-compartment electrochemical cell comprised of the chemically-modified electrode as a working electrode, a glassy carbon auxiliary electrode isolated by a glass frit, and a saturated calomel electrode (SCE) connected to the working volume with a Luggin capillary. All potentials are reported with respect to this reference electrode. Argon bubbling was used to remove oxygen from the solutions in the electrochemical cell. During the measurements the cell was thermostated (35 °C).

Chemical Modification of Electrodes. (a) Electrode pretreatment and deposition of the cystamine monolayer: To remove any previous organic layer associated with the Au-electrodes and to regenerate a bare metal surface, the electrodes were treated with a boiling 2 M solution of KOH for 1 h, rinsed with water, and stored in concentrated sulfuric acid. Immediately before modification, the electrodes were rinsed with water, soaked for 10 min in concentrated nitric acid, and then rinsed with water again. The clean bare gold electrode was soaked in a 0.02 M cystamine solution in water for 2 h. The electrode was then rinsed thoroughly with water to remove any physically adsorbed cystamine.

(b) Preparation of antigen monolayer-modified electrodes consisting of Nϵ-2,4-dinitrophenyl-L-lysine, **3**, or 3,5-dinitrosalicylic acid, **4**, antigens. The cystamine monolayer-modified Au-electrode was soaked for 3 h in a 0.01 M HEPES buffer solution, pH = 7.3, that included Nϵ-2,4-dinitrophenyllysine, 3 mM, and 1-ethyl-3-(3-dimethylaminopropyl) carbodiimide (EDC, Aldrich), 10 mM (as a coupling reagent).

Attachment of **4** was accomplished as described for **3**. Attachment of a dinitrospiropyran antigen was done by soaking a clean bare Au electrode in a 20 mM mercaptobutyl dinitrospiropyran, **1**, solution in DMF for 2 h. The electrode was then washed with DMF to remove any physically adsorbed mercaptobutyl dinitrospiropyran.

QCM measurements were performed with a quartz crystal analyzer (EG&G Model QCA917) connected to a PC. For QCM measurements, quartz crystals, 9 MHz (AT-cut, EG&G) sandwiched between two Au electrodes (A = 0.186 cm^2, roughness factor ca. 3.5) were used. The fundamental frequency of the crystals was ca. 9×10^6 Hz.

Light-Induced Photoisomerization of Photoactive Antigen Monolayers. For the generation of the dinitrospiropyran monolayer configuration, SP-state, the Au electrode was irradiated at $\lambda > 495$ nm, at ambient atmosphere using a 150W xenon lamp, Oriel, equipped with a filter ($\lambda > 495$ nm). For the generation of the dinitromerocyanine monolayer electrode, MRH^+-configuration, the surface was irradiated at $360 < \lambda < 380$ nm, for 5 min, at ambient atmosphere using a Hg pencil lamp source (Oriel, 6042, long wave filter) held 1 cm from the surface of the electrode.

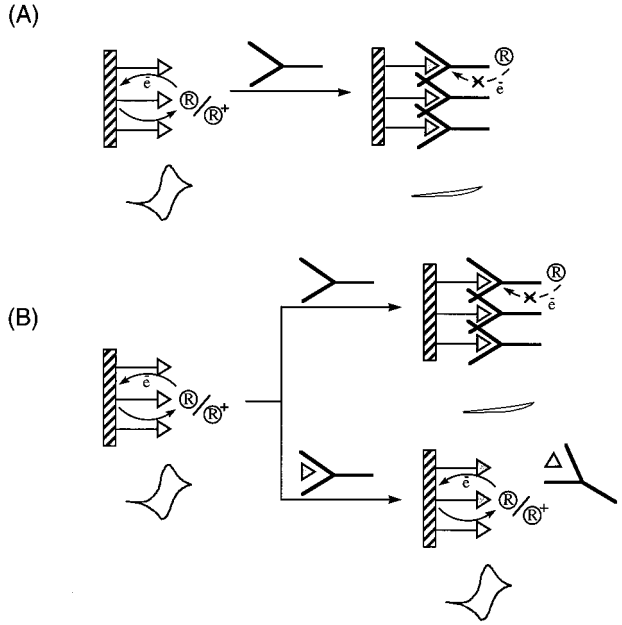

Figure 1. (A) Electrochemical analysis of an antibody by an antigen monolayer-modified electrode, using a redox probe in the electrolyte solution. (B) Electrochemical analysis of an antigen by an antigen monolayer electrode in the presence of a constant antibody concentration.

Results and Discussion

Amperometric Antigen-Monolayer Immunosensors. The concept of an amperometric antibody sensor is shown in Figure 1A. The antigen is organized on the electrode as a monolayer. The redox couple, R^+/R is present in the electrolyte solution, and the antigen monolayer electrode yields an amperometric response upon application of the appropriate potential that oxidizes (or reduces) the redox probe in solution. Interaction of the antigen monolayer electrode with the respective antibody, Ab, results in the association of the Ab to the monolayer and the insulation of the electrode toward the redox probe. The extent of electrode insulation depends on the Ab-concentration in the analyzed solution and time of incubation of the monolayer with the Ab solution. Thus, the decrease in amperometric (or coulometric) response of the antigenic monolayer electrode, upon interaction with the respective Ab solution for a fixed time, provides a quantitative measure to the Ab concentration. Scheme 1 shows the assembly of a dinitrophenyl antigen monolayer on the Au electrode surface: cystamine was self-assembled onto a Au electrode as a base monolayer. Reaction of the monolayer-substituted electrode with Nϵ-2,4-dinitrophenyl-L-lysine, **3**, results in the respective dinitrophenyl-substituted monolayer. The surface density of the primary amine monolayer was determined by reacting the cystamine-modified monolayer electrode with pyrroloquinoline quinone (PQQ) and coulometric analyses of the covalently linked quinone units. The surface density is estimated to be $\sim 1 \times 10^{-10}$ mol·cm^{-2}. This value should be considered as a lower limit value for the surface coverage with the amino groups, since complete modification of the monolayer with the quinone units is assumed. This monolayer electrode acts as an antigenic surface for *anti*-DNP-Ab. Accordingly, the amperometric response of the antigen-monolayer electrode in the electrochemical cell that includes $K_4Fe(CN)_6$ as redox probe was recorded at different *anti*-DNP-Ab concentrations. Figure 2, curve b, shows the cyclic voltammogram of the monolayer electrode in the presence of $K_4Fe(CN)_6$. A reversible cyclic voltammogram is observed, indicating that the redox probe exhibits electrical communication

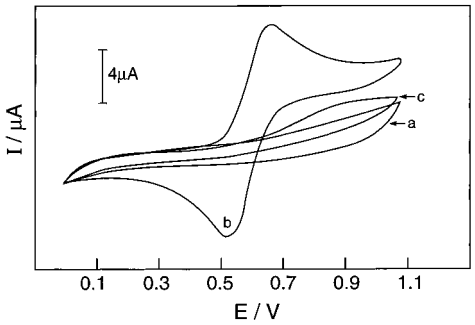

Figure 2. Cyclic voltammograms of Nϵ-2,4-dinitrophenyl-L-lysine, **3**, monolayer electrode: (a) In the presence of the background electrolyte composed of 0.1 M buffer, pH = 7.0. (b) Upon addition of $[K_3Fe(CN)_6] = 1.1 \times 10^{-3}$ M to the electrolyte solution. (c) Upon treatment of the electrode with the *anti*-DNP-Ab, 15 μM for 5 min, at 35 °C. For all experiments scan rate 100 mV·s^{-1}.

with the antigen monolayer electrode. Figure 2, curve c shows the cyclic voltammogram of the antigen monolayer in the presence of $K_4Fe(CN)_6$, after treatment with the *anti*-DNP-Ab (5 μM, 35 °C, 6 min). The electrical communication between the redox probe and the electrode decreases and becomes irreversible. This is attributed to the association of the bulky *anti*-DNP-Ab to the antigenic monolayer electrode, which perturbs the electrical contact and electron transfer rate between the $K_4Fe(CN)_6$ and the electrode surface. The difference between the amperometric signals of the antigen electrode by itself, and that of the antigen electrode treated with variable concentrations of *anti*-DNP-Ab, Δi_{pc}, indicates the extent of the electrode insulation. The value Δi_{pc} increases as the *anti*-DNP-Ab concentration is elevated, and antibody concentrations as low as 0.5 μM can be detected by this monolayer antigen-electrode. (The respective calibration curve is given as Supporting Information.)

The antigen monolayer electrode allows also the amperometric analysis of the antigen itself. This process is schematically exemplified in Figure 1B, where two extreme conditions are discussed. To the analyzed antigen solution a constant concentration of the respective antibody is added. In the absence of the antigen in the analyte solution, the antibody remains in its free state. Challenging of the antigenic monolayer electrode with the probe solution will result in the insulation of the electrode surface, and its electrical response will be blocked. On the other hand, at a high antigen concentration in the analyte sample, the antibody is blocked by the antigen. Interaction of the analyte sample with the antigen monolayer-electrode will not lead to its electrical insulation. Thus, a high antigen content in the analyte solution will be reflected by a high amperometric response of the functionalized electrode. Note that the concentration of the antibody used in order to probe the antigen must be tuned to the desired concentration range of the antigen in the analyte sample. As *anti*-DNP-Ab includes two binding sites for the dinitrophenyl antigen in the F_{ab} region, the molar ratio of the probe antibody in the analyte sample should be less than half of the planned sensitivity range of the antigen. Accordingly, the Nϵ-2,4-dinitrophenyl-L-lysine, **3**, monolayer electrode was applied to sense **3** in the presence of *anti*-DNP-Ab. Figure 3, curve b, shows the cyclic voltammogram of the antigenic monolayer electrode in the presence of $K_4Fe(CN)_6$. The redox probe reveals a reversible redox-wave implying unperturbed electrical communication with the electrode surface. Figure 3, curve c, shows the cyclic voltammogram of the antigenic monolayer electrode in the presence of $K_4Fe(CN)_6$ after treatment with a solution which contains the *anti*-DNP-Ab (5 μM) and the antigen (**3**) (100 μM) for 6 min at 35 °C.

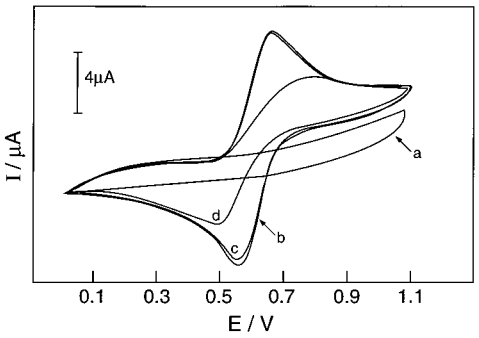

Figure 3. Cyclic voltammograms of **3**-monolayer electrode: (a) In the presence of background electrolyte composed of 0.1 M buffer, pH = 7.0. (b) Upon addition of $[K_3Fe(CN)_6] = 1.1$ mM to the electrolyte. (c) Upon treatment of the electrode with the analyte solution which contains **3**, 100 μM, and *anti*-DNP-Ab, 5 μM for 5 min at 35 °C. (d) Upon treatment of the electrode with the analyte solution which contains *anti*-DNP-Ab, 5 μM, but does not contain **3**, for 5 min at 35 °C. For all experiments scan rate 100 mV·s^{-1}.

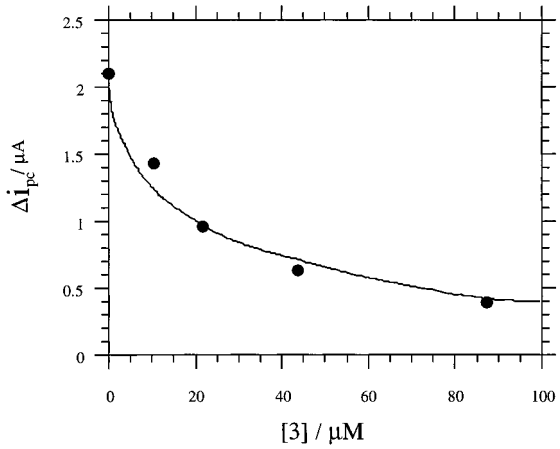

Figure 4. Amperometric responses of **3**-monolayer-electrodes at different concentrations of **3**. In all experiments the *anti*-DNP-Ab concentrations in the probe solution corresponds to 50 μM. The amperometric responses were recorded after treating the electrode for 5 min with the analyte solution. Amperometric responses (ΔI_{pc}) are expressed as the difference between the amperometric response of the monolayer electrode (at $E = 0.5$ V) in the electrolyte solution and the amperometric response after treatment of the electrode with the analyte solution containing the *anti*-DNP-Ab and a given concentration of the antigen. All measurements were performed in 0.1 M phosphate buffer, pH = 7.0, $[K_3Fe(CN)_6] = 1.1 \times 10^{-3}$ M, at 35 °C, scan rate = 100 mV·s^{-1}.

No change in the electrical communication of $K_4Fe(CN)_6$ was observed. Figure 3, curve d, shows the cyclic voltammogram of the electrode, in the presence of $K_4Fe(CN)_6$, after treatment with a solution which contains the *anti*-DNP-Ab (5 μM) and the antigen (**3**) at a low concentration (10 μM) for 6 min at 35 °C. A decrease in the amperometric response was recorded, due to the partial insulation of the antigenic monolayer by the *anti*-DNP-Ab. Figure 4 shows the calibration curve of the electrode responses at different antigen (**3**) concentrations. (Δi_{pc} is defined as the difference between the amperometric response of the antigen monolayer electrode in the presence of the redox probe only and the response of the electrode at constant Ab concentration (5 μM) and variable antigen concentrations.) Antigen concentrations between 10 and 100 μM were detected by this antigenic monolayer electrode at a constant antibody concentration that equals to 5 μM.

The electrochemical detection of an antibody (or an antigen) by the antigen monolayer electrode was based on the extent of the electrode insulation toward a molecular redox probe

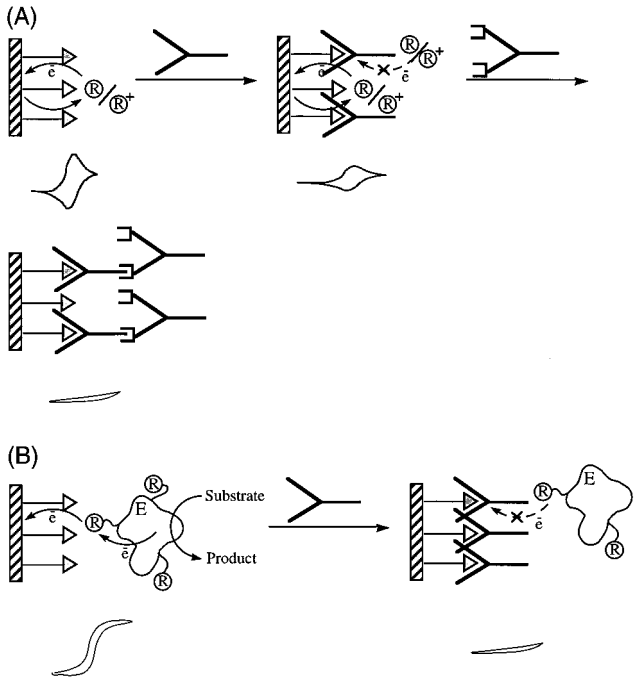

Figure 5. (A) Schematic amperometric analysis of an antibody by an antigen monolayer-electrode in the presence of a redox-probe using the *anti*-antibody for enhanced insulation. (B) Schematic amperometric analysis of an antibody by an antigen-monolayer electrode, using a bioelectrocatalyst as redox probe.

solubilized in the electrolyte. This effect of insulation of the electrode interface originates from the formation of the antigen−antibody complex at the electrode surface. The molecular redox probe used in these studies was the $Fe(CN)_6^{3-}/Fe(CN)_6^{4-}$ redox-couple. The changes in the amperometric responses of the molecular redox probe, as a result of binding the high-molecular-weight antibody to the electrode surface, are, however, quite small in their magnitude. Furthermore, we find that the amperometric responses of the tailored functionalized-electrode in the presence of the antibody are very sensitive to the quality of the antigen monolayer. That is, any defects or "pinholes" in the antigen monolayer assembly results in difficulties in probing the insulation of the electrode. These difficulties are reflected by significant alterations in the extent of insulation of surfaces functionalized by the antigen at different preparations. The observed Δi_{pc} values for different electrode preparations vary within the range ±15%. We applied two different strategies in order to overcome these difficulties: One approach involves the increase of the mass of the antibody associated with the antigen monolayer by using the respective *anti*-antibody (in addition to the antibody itself). Thus, the binding of the high molecular-weight *anti*-antibody to the base monolayer of the Ab associated with the electrode is expected to enhance the insulation of the functionalized electrode. This is anticipated to increase the sensitivity of the sensing interface and to screen or mask any structural defects in the primary, low molecular-weight, antigen monolayer. In the second approach, we applied an "electrically-wired" redox enzyme, i.e., ferrocene-functionalized glucose oxidase (Fc-GOx) as a bulky redox probe that amplifies the antigen antibody interaction at the electrode surface. The redox-enzyme is insensitive to molecular defects in the monolayer assembly, and hence the electrode response should be insensitive to such structural perturbations.

The concept of amplifying the extent of the electrochemical insulation by using the *anti*-antibody is shown in Figure 5A. The antigen is assembled onto the electrode surface. Challenging of the antigenic monolayer electrode with the antibody

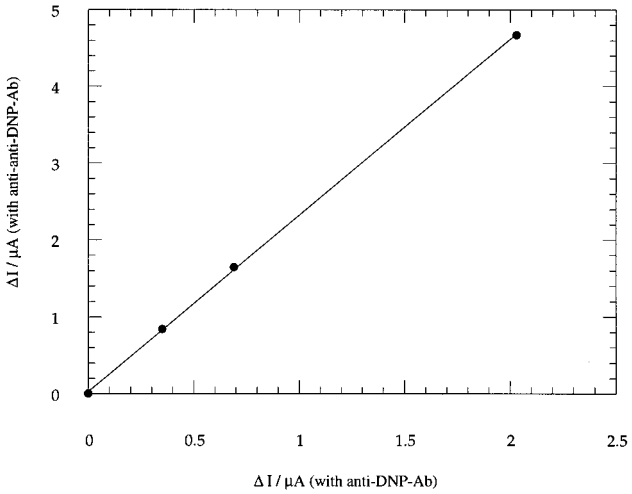

Figure 6. Amplified amperometric transduction of the formation of the *anti*-DNP-Ab/antigen monolayer complex at the electrode surface, using the *anti*−*anti*-DNP-Ab for enhanced insulation of the electrode. The redox probe is $[K_3Fe(CN)_6] = 1.1 \times 10^{-3}$ M. Plot shows the extent of electrode insulation by the *anti*-Ab and *anti*-DNP-Ab complex vs the electrode insulation by the DNP-Ab alone.

solution results in the partial electrochemical insulation of the electrode surface toward the redox probe R^+/R that is present in the electrochemical cell. Further treatment of the same electrode with *anti*-antibody solutions increases the electrochemical insulation of the electrode toward the reduction or the oxidation of the redox probe R^+/R. The *anti*-DNP-Ab is a monoclonal IgE antibody produced in mice. We used *anti*-mouse IgE (epsilon chain, produced in goat) as the *anti*-Ab. Figure 6 shows the amplification of the amperometric sensing of the *anti*-DNP-Ab by the application of the *anti*-Ab and use of the dinitrophenyllysine antigen monolayer as sensing interface and $K_4Fe(CN)_6$ as a redox probe. In this figure, the extent of electrode insulation, Δi_{pc} values, observed upon interaction of the antigen-monolayer-electrode at variable concentrations of the *anti*-DNP-Ab (interaction time 10 min) is plotted as a function of the magnitude of electrode insulation, Δi_{pc} values, of the electrodes treated with the *anti*-DNP-Ab and the *anti*-Ab (interaction time 10 min, constant concentration of 10 $\mu g \cdot mL^{-1}$). Note that each point in this plot corresponds to a different concentration of the parent *anti*-DNP-Ab. The slope of this plot is ca. 2.5, implying that the extent of the electrode insulation in the presence of the *anti*-Ab is ca. 2.5-fold higher than that observed with the *anti*-DNP-Ab by itself. Thus, the sensitivity of the antigen monolayer electrode for the *anti*-DNP-Ab is substantially enhanced by the application of the secondary electrode treatment with the *anti*-Ab.

The concept of utilizing a redox enzyme to probe the association of an antibody to an antigen monolayer electrode is schematically outlined in Figure 5B. The antigen monolayer is assembled on the electrode surface, and a redox relay-modified enzyme is used to probe the interactions of the antibody with the antigenic monolayer electrode. Chemical modification of redox-enzymes by electron-relay units yields "electrically wired" enzymes that communicate with the electrode surfaces.[37] The redox-relay units act as electron mediators for charge transport between the enzyme redox site and the electrode surface. In the presence of the antigen monolayer electrode, electrical communication between the modified enzyme and the electrode exists. This leads to the bioelectrocatalyzed oxidation of the enzyme substrate and the formation

(37) Blonder, R.; Katz, E.; Cohen, Y.; Itzhak, N.; Riklin, A.; Willner, I. *Anal. Chem.* **1996**, *68*, 3151.

Scheme 1. Assembly of a Nϵ-2,4-Dinitrophenyl-L-lysine, **3**, Monolayer onto a Au-Electrode

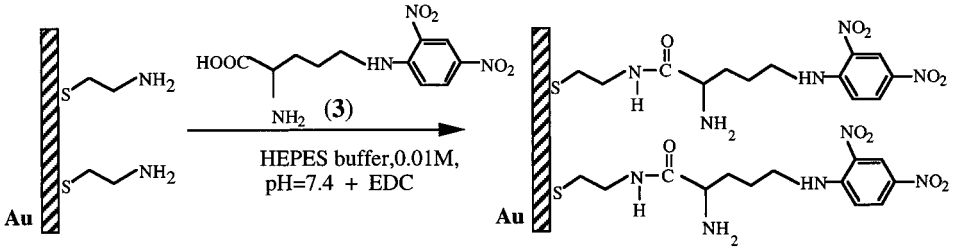

Scheme 2. Modification of Glucose Oxidase, GOx, by *N*-Methylferrocene Caproic Acid, **2**

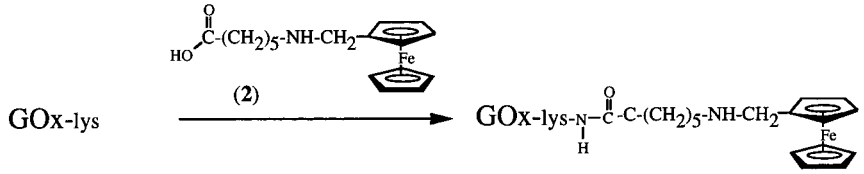

of an electrical current by the electrode. Interaction of the monolayer-modified electrode with the antibody results in the formation of the antigen−antibody complex on the electrode surface. The bulky structure of the antibody perturbs the electrical communication between the redox protein and the electrode and inhibits the biocatalytic reaction of the enzyme. The extent of electrode insulation by the antibody is controlled by its bulk concentration in the analyte sample and the time of incubation. The use of an "electrically-wired" enzyme as a redox probe to follow the formation of the antigen−Ab at the electrode interface has two advantages in comparison to the previously discussed method applying the molecular redox probe R^+/R:

(i) The high molecular-weight biocatalyst is insensitive to microscopic defects or "pinholes" in the antigen-monolayer assembly, and (ii) the redox-enzyme amplifies the antigen−antibody interactions at the electrode surface by producing a bioelectrocatalytic current.

This electrode configuration that includes the dinitrophenyllysine antigen monolayer, Scheme 1, was used for the electrochemical sensing of the *anti*-DNP-Ab. The redox biocatalyst employed to sense the formation of the antigen−antibody complex at the monolayer interface was glucose-oxidase, GOx, modified by *N*-(2-methylferrocene) caproic acid, **2**, as electron mediator units, Fc-GOx. Previous studies indicated that covalent attachment of electron relay units, and specifically, ferrocene units covalently tethered to GOx, yield a biocatalyst that electrically communicates with electrode surfaces.[38] In these systems, electrochemical oxidation of the redox units, tethered to the external protein periphery, allows electron transfer with intraprotein redox relay units, and the oxidation of the protein-embedded flavin cofactor. This electron transfer path facilitates electrical contact between the biocatalyst redox center and the electrode and induces the bioelectrocatalyzed oxidation of glucose. GOx was modified by *N*-(2-methylaminoferrocene) caproic acid, **2**, Scheme 2. The average loading of the protein with the ferrocene units corresponds to 21. Figure 7, curve b, shows the cyclic voltammogram of the antigen-monolayer-electrode in the presence of Fc-GOx and glucose. An electrocatalytic anodic current is observed at the redox-potential characteristic to the ferrocene units, indicating that the modified enzyme exhibits electrical communication with the antigenic monolayer electrode. This stimulates the electrobiocatalytic oxidation of glucose. Figure 7, curve c, shows the cyclic voltammogram of the antigen monolayer electrode in the presence of Fc-GOx and glucose, after treatment with the *anti*-DNP-Ab (50 $\mu g \cdot mL^{-1}$, 6 min). The electrical communication between the redox-modified enzyme and the electrode is entirely blocked, and only the background response of the electrolyte solution is observed. This is attributed to the association of the bulky *anti*-DNP-Ab to the monolayer electrode, which prevents the electrical contact between the Fc-GOx and the electrode surface. Figure 7, curve d, shows the cyclic voltammogram of the antigen-monolayer-electrode after treatment with the *anti*-DNP-Ab and in the presence of Fc-GOx but upon addition of the diffusional electron mediator ferrocenecarboxylic acid. An electrocatalytic anodic current is observed that is only slightly lower in magnitude than that of the freshly prepared antigen-monolayer-electrode. Thus, in the presence of the low-molecular-weight electron mediator, diffusion of the ferrocenecarboxylic acid through the monolayer "pinholes" provides

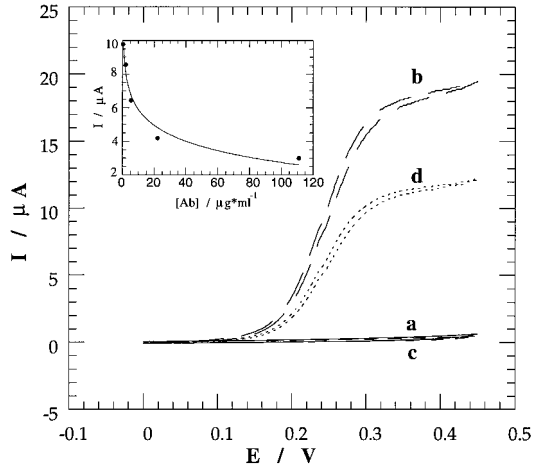

Figure 7. Cyclic voltammograms of **3**-monolayer-electrode: (a) In the presence of the background electrolyte composed of 0.1 M phosphate buffer, pH = 7.0. (b) Upon addition of ferrocene-modified GOx, Fc-GOx, 4 $mg \cdot mL^{-1}$, and glucose, 0.05 M, to the electrolyte solution. (c) Upon treatment of the electrode with *anti*-DNP-Ab, 50 $\mu g \cdot mL^{-1}$ for 6 min and in the presence of Fc-GOx and glucose. (d) With *anti*-DNP-Ab treated electrode and upon addition of ferrocene carboxylic acid, 5×10^{-4} M, as diffusional electron mediator, to the electrolyte solution that includes Fc-GOx and glucose. For all experiments scan rate 2 $mV \cdot s^{-1}$, temperature 35 °C. (inset): Amperometric responses of **3**-monolayer electrode upon its interaction with different *anti*-DNP-Ab concentrations. All data were recorded by chronoamperometry (4.5 s after potential step from 0 to 0.5 V) in 0.01 M phosphate buffer, pH = 7.0, in the presence of Fc-GOx, 5 $mg \cdot mL^{-1}$, and glucose, 0.05 M. Electrodes were incubated with the *anti*-DNP-Ab solutions of the respective concentrations for 30 min.

(38) Degani, Y.; Heller, A. *J. Phys. Chem.* **1987**, *91*, 1285.

Scheme 3. Assembly of a 3,5-Dinitrosalicylic Acid, **4**, Monolayer onto a Au-Quartz Electrode

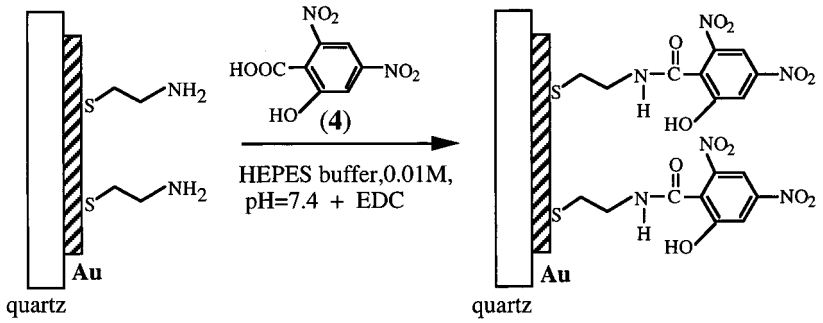

electrical communication between the redox enzyme and the electrode. This yields the electrocatalytic anodic current even in the presence of the antigen−antibody complex at the electrode interface. Figure 7 (inset) shows the decrease in the amperometric responses of the antigen monolayer electrode at different *anti*-DNP-Ab concentrations using Fc-GOx and glucose as a redox probe to follow the formation of the antigen−antibody complex. The current responses decrease as the concentration of the *anti*-DNP-Ab increases, and the amperometric signal is totally blocked at *anti*-DNP-Ab concentration of 50 $\mu g \cdot mL^{-1}$ (incubation time 6 min). The antigen monolayer electrode is thus an active interface for electrochemical detection of the *anti*-DNP-Ab in the concentration range of 2−50 $\mu g \cdot mL^{-1}$.

Microgravimetric, Piezoelectric, Antigen-Monolayer Immunosensors. In the previous section, the association of the antibody to the antigen monolayer was sensed indirectly by following the electrical insulation of the electrochemical response of a redox-probe upon the formation of the antigen−antibody complex at the electrode surface. Recent studies of our laboratory reported the microgravimetric, piezoelectric, transduction of the formation of antigen−antibody complexes at functionalized quartz crystals. It was demonstrated that the modification of Au-electrodes, associated with a piezoelectric quartz crystal, with an antigen monolayer, i.e., fluorescein or α-D-mannopyranose, yield active interfaces for the microgravimetric analysis of the *anti*-fluorescein-Ab or of the concanavalin A receptor, respectively.[24,37] This generic method to sense antigen−antibody interactions was further applied by us to develop a piezoelectric-based immunosensor for the *Chlamydia trachomatis* bacteria.[39] The theory involved with the factors dominating the resonance frequencies of piezoelectric crystals and the feasibility of following chemical transformations at the crystal surfaces by microgravimetric analyses was extensively reviewed. The use of piezoelectric quartz crystals for the microgravimetric, quartz-crystal-microbalance, QCM, analysis of antigen−antibdoy interactions was addressed in several reports[40,41] and reviews.[42−44] The frequency change of the quartz crystal, Δf, upon a mass alteration of Δm occurring on the crystal, is given by eq 1, where f_o is the fundamental frequency of the crystal, n is the overtone number ($n = 1$), ρ_q is the density of the quartz (2.65 $g \cdot cm^{-2}$), and μ_q is the shear modulus of quartz (2.95×10^{11} dyne cm^{-2}). For the quartz crystals used in the present study, AT-cut, 9 MHz, $C_f = 1.83 \times 10^8$ ($Hz \cdot cm^2 \cdot g^{-1}$). Thus, by the assembly of the antigen monolayer on Au-electrodes associated with a quartz crystal, mass changes on the crystal, resulting from the antibody association, can be directly identified by following the frequency changes of the crystal.

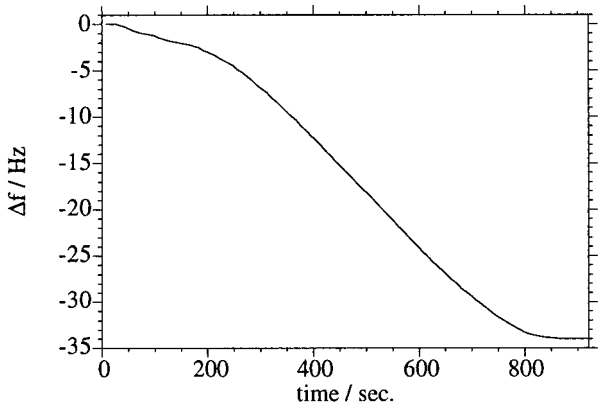

Figure 8. Time-dependent frequency changes of a dinitrosalicyl acid monolayer assembled onto a Au quartz crystal according to Scheme 3, in the presence of *anti*-DNP-Ab 25 $\mu g \cdot mL^{-1}$. The experiment was recorded in PBS buffer.

$$\Delta f = -\left[\frac{2nf_o^2}{(\mu_q r_q)^{1/2}}\right]\Delta m = -C_f \Delta m = -1.83 \times 10^8 \ (Hz \cdot cm^2 \cdot g^{-1})\Delta m \quad (1)$$

The formation of the antibody−antigen complex was associated with a mass increase on the crystal that is reflected by a decrease in the resonance frequency of the crystal. Scheme 3 shows the assembly of a 3,5-dinitrosalicylic acid, **4**, monolayer on a Au-electrode, resulting in a dinitrophenyl-antigen functionalized monolayer. The surface density of the 3,5-dinitrosalicylic acid derivative on the Au-electrodes associated with the quartz crystal was determined by following the crystal frequency change upon coupling of **4** to the base cystamine monolayer. The observed frequency change is $\Delta f = -100$ Hz, and the corresponding surface coverage of the antigen is $\sim 6 \times 10^{-10}$ $mol \cdot cm^{-2}$. Figure 8 shows the frequency changes of the antigen-functionalized crystal upon injection of 25 $\mu g \cdot mL^{-1}$ of *anti*-DNP-Ab. The decrease in the crystal frequency, $\Delta f = -35$ Hz, indicates an increase in the crystal mass as a result of the Ab association to the antigen-monolayer-functionalized crystal. The time-dependent frequency decrease reflects the dynamics of association of the antibody to the antigen interface. The constant value of decreased, leveled-off, frequency represents the equilibrium state of associated Ab to the surface. From the frequency change of the crystal the surface coverage of the DNP-Ab on the antigen monolayer is estimated to be $\sim 4 \times 10^{-13}$ $mol \cdot cm^{-2}$ (M.W. of *anti*-DNP-Ab is ca. 220 000 $g \cdot mol^{-1}$).

The antigen-monolayer-functionalized crystal enables also the microgravimetric quartz-crystal-microbalance analysis of the

(39) Ben-Dov, I.; Willner, I.; Zisman, E. *Anal. Chem.* **1997**, *69*, 3506.
(40) Konig, B.; Grätzel, M. *Anal. Chem.* **1994**, *66*, 341.
(41) Wagner, G.; Guilbault, G. G. In *Food and Biosensor Analysis*; Marcel Dekker, Inc., New York, 1994; pp 151−172.
(42) Konig, B.; Grätzel, M. *Anal. Chim. Acta* **1993**, *276*, 329.
(43) Ward, M. D.; Buttry, D. A. *Science* **1990**, *249*, 1000.
(44) Bard, A. J. *Electroanalytical Chemistry*; Marcel Dekker, Inc.: New York, 1991; Vol. 17, pp 1−85.

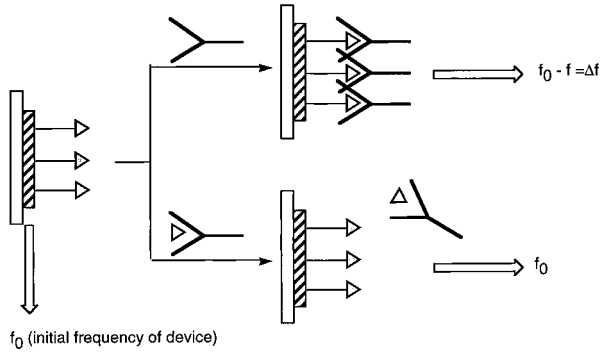

Figure 9. Competitive analysis of an antigen by an antigen monolayer associated with a quartz crystal using a fixed amount of Ab to probe the antigen in the analyte sample.

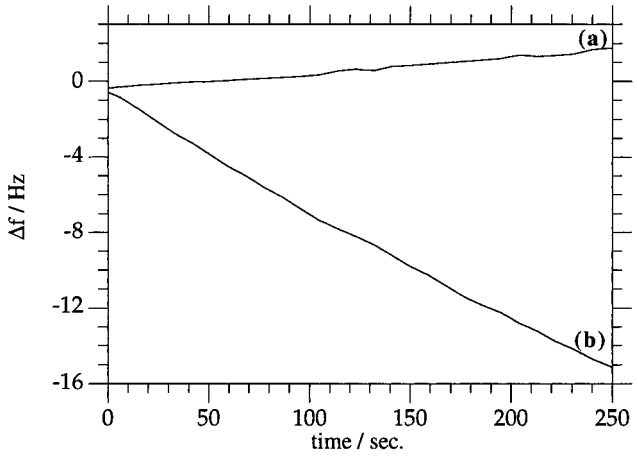

Figure 10. Time-dependent frequency changes of a crystal that includes dinitrosalicylic acid, **4**, as antigen monolayer assembled onto a Au-quartz in the presence of (a) *anti*-DNP-Ab, 20 mg·mL^{-1} and 2,4-dinitrophenyl, 40 pg·mL^{-1} in the analyte sample and (b) only *anti*-DNP-Ab, 20 ng·mL^{-1} in the analyte sample. The experiments were recorded in PBS buffer.

antigen itself, as schematically outlined in Figure 9. The antigen-monolayer-modified crystal is challenged with an analyte sample that includes a fixed and constant concentration of the Ab. The concentration of the probe-Ab should be lower than the detection limit requested for the antigen and should take into account the number of epitope sites in the F_{ab} region. Thus, in the absence of the antigen in the analyte sample, the Ab remains free. Upon interaction of the sample with the antigen-monolayer-functionalized crystal, association of the antibody to the antigen interface proceeds, and the process is reflected by a frequency decrease of the crystal. A sample that includes the analyte-antigen will result in the association of the antigen to the probe-Ab. Challenging of the sample with the antigen-functionalized crystal will not stimulate any significant frequency change since the antibody is in a bound configuration. Accordingly, the 3,5-dinitrosalicylic acid monolayer functionalized crystal was applied to sense 2,4-dinitrophenol in the presence of the *anti*-DNP-Ab. Figure 10, curve a, shows the frequency changes of the antigen-modified crystal upon treatment with a solution that contains the *anti*-DNP-Ab (20 ng·mL^{-1}) and the analyte-antigen 2,4-dinitrophenol (40 pg·mL^{-1}). No change in the frequency is observed, implying that no significant mass change at the crystal interface occurred. Figure 10, curve b, shows the frequency changes of the monolayer-modified crystal upon treatment with an analyte solution that contains only the *anti*-DNP-Ab. A decrease in the crystal

(45) Guglielmetti, R. In *Photochromism: Molecules and Systems*; Dürr, H., Bouas-Laurent, H., Eds.; Elsevier: Amsterdam, 1990; pp 314−466.

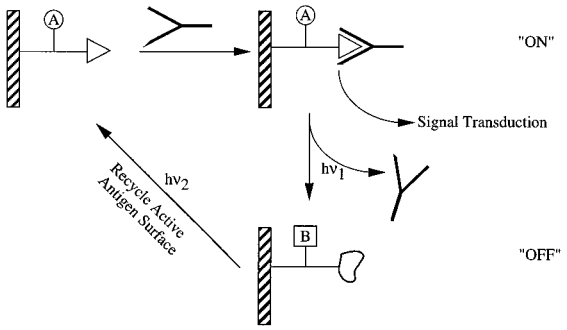

Figure 11. Schematic configuration of a reversible immunosensor device using a photoisomerizable antigen monolayer assembled on a transducing support as a functionalized interface for sensing the Ab and photochemical regeneration of the sensing surface.

frequency is recorded ($\Delta f = -15$ Hz), indicating the association of the free antibody to the antigen monolayer. Thus, the interaction of an antibody probe solution with a molecular analyte provides an extremely sensitive analytical detection method for the molecular antigen-analyte.

Reversible Amperometric and Piezoelectric Immunosensors. The tight antigen−antibody interactions turn the electrochemical or piezoelectric immunosensing surfaces into single-cycle devices. The strong association of the antibodies to the antigen layer and the deactivation of the surface by the occupation of the antigen sensing sites represents a basic disadvantage in the immunosensor technology. The treatment of antigen−antibody interfaces at high ionic strength or acidic pH values provides a means to dissociate the antigen−antibody complex and, eventually, allows the regeneration of the sensing antigen interface. These methods are limited, however, as the extreme conditions often chemically degrade or deactivate the antigen interface. Also, the extreme pH or ionic strength variations are often not sufficient to dissociate the antigen−antibody complex. The concept of photochemical regulation of biorecognition phenomena and biospecific interactions was developed in our laboratory in recent years.[27−31] Reversible photoisomerizable groups linked to the biomaterials provide a means to photocontrol their functions. In one photoisomer state, the biomaterial structure is perturbed and its biological functions are inhibited, whereas in the complementary photoisomer state the biomaterial retains the bioactive structure and its biochemical function is activated. For example, this approach was successfully applied to photostimulate the association of D-mannopyranose to concanavalin A modified by nitrospiropyran units.[28]

Figure 11 shows the schematic adaptation of the principle of light-stimulated control of biomolecular recognition phenomena to tailor reversible immunosensor devices. The antigen monolayer immobilized onto the electrode is modified by photoisomerizable units. In the photoisomer state A the antigen exhibits affinity for the antibody and allows the electrochemical or the microgravimetric transduction of the Ab association to the monolayer. After completion of the first analysis cycle, the monolayer electrode is photoisomerized to state B. The original antigen units are sterically perturbed to a structure lacking affinity for the Ab. This enables one to wash-off the Ab from the sensing surface. By reversible, light-stimulated, isomerization of the monolayer from state B to A, the active antigen monolayer is regenerated. Thus, by a two-step irradiation of the monolayer interface, the antibody sensing electrode is recycled. This principle for tailoring reversible immunosensing devices was demonstrated with the development of a reversible antigen-electrode for the analysis of the dinitrophenyl antibody, *anti*-DNP-Ab. Spiropyran compounds, i.e., dinitrospiropyran, exhibit reversible photoisomerizable properties,[45] eq

Scheme 4. Assembly of Mercaptobutyl Dinitrospiropyran, **1**, onto a Au-Electrode To Generate a Photoisomerizable Antigen Monolayer Electrode

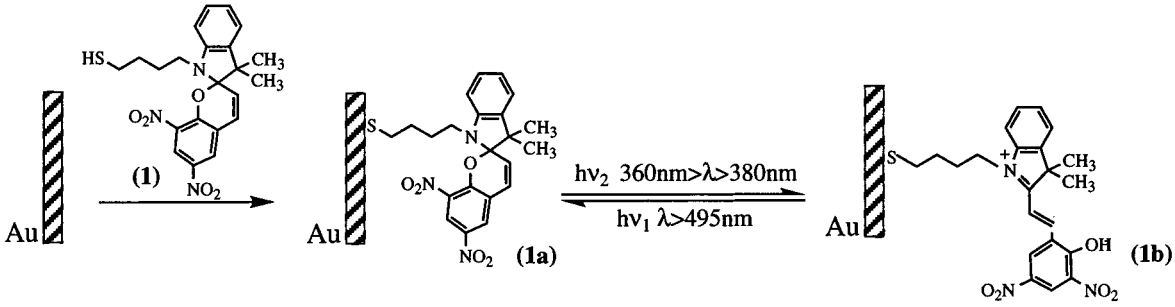

2. It has been shown that the two photoisomer states of dinitrospiropyran and dinitromerocyanine exhibit different affinities for the *anti*-DNP-Ab. Dinitrospiropyran derivatives act as antigens for the *anti*-DNP-Ab, but the dinitromerocyanines lack affinity and binding properties to the *anti*-DNP-Ab.[23]

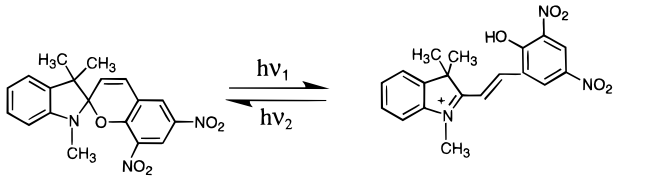

(2)

Accordingly, we assembled the mercaptobutyl dinitrospiropyran, **1**, as monolayer on a Au-electrode, Scheme 4. The monolayer exhibits reversible photoisomerizable properties. Irradiation of the dinitrospiropyran monolayer, SP-state, $360 < \lambda < 380$ nm, results in the protonated merocyanine isomer monolayer, MRH^+-state, where further illumination of the MRH^+-monolayer interface, $\lambda > 495$ nm, regenerates the SP-monolayer. The surface density of the **1** monolayer was determined by the coulometric analysis of the aromatic nitro groups[46] and is estimated to be $\sim 4 \times 10^{-11}$ mol·cm^{-2}. Figure 12 shows the cyclic voltammograms of the dinitrospiropyran monolayer electrode, SP-state, in the absence of the *anti*-DNP-Ab (curve a) and in the presence of the *anti*-DNP-Ab (curve b) using Fc-GOx and glucose as redox probe to follow the Ab association to the monolayer electrode. In the presence of the dinitrospiropyran monolayer electrode, effective electrical contact between Fc-GOx and the electrode exists, giving rise to a high electrocatalytic anodic current resulting from the bioelectrocatalyzed oxidation of glucose. Treatment of the dinitrospiropyran monolayer electrode with the *anti*-DNP-Ab blocks the electrobiocatalyzed oxidation of glucose (curve b). Association of the *anti*-DNP-Ab to the antigen monolayer prevents the electrical communication between Fc-GOx and the electrode, and, consequently, the bioelectrocatalyzed oxidation of glucose is eliminated. Photoisomerization of the dinitrospiropyran monolayer electrode to the protonated dinitromerocyanine monolayer electrode, MRH^+-state, without the *anti*-DNP-Ab and in the presence of Fc-GOx and glucose, results in the electrochemical response shown in Figure 12 (curve c). A slightly higher electrocatalytic anodic current as compared to the SP-monolayer electrode is observed. This is attributed to the electrostatic

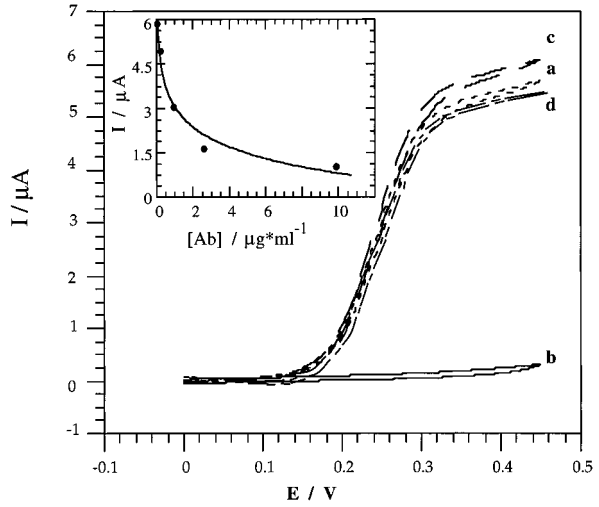

Figure 12. Cyclic voltammograms of the dinitrospiropyran photoisomerizable monolayer electrode in the presence of Fc-GOx, 5 mg·μL^{-1}, and glucose, 50 mM: (a) In the presence of the **1a**-monolayer electrode, SP-state. (b) In the presence of the **1a**-monolayer electrode after treatment with the *anti*-DNP-Ab solution, 0.15 mg·mL^{-1}, for 6 min. (c) In the presence of the protonated **1b**-monolayer electrode, MRH^+-state. (d) In the presence of the **1b**-monolayer electrode after treatment with *anti*-DNP-Ab solution, 0.15 mg·mL^{-1}, for 6 min. All experiments were performed in 0.1 M phosphate buffer solution, pH = 7.0, under argon, 35 °C, scan rate = 5 mV·s^{-1}. The SP-monolayer state was generated by irradiation of the electrode, $\lambda > 495$ nm. The MRH^+-monolayer electrode was generated by irradiation of the SP-electrode, $360 \text{ nm} < \lambda < 380$ nm. (inset): Amperometric responses of the **1a**-monolayer electrode at different *anti*-DNP-Ab concentrations. Data recorded in 0.1 M phosphate buffer, pH = 7.0, under argon, 35 °C, and in the presence of Fc-GOx 5 mg·mL^{-1} and glucose, 50 mM, scan rate = 5 mV·s^{-1}.

attraction of Fc-GOx to the positively charged MRH^+-monolayer electrode. Concentration of the biocatalyst at the electrode interface enhances the bioelectrocatalyzed oxidation of glucose, resulting in the slightly higher amperometric response. Treatment of the MRH^+-monolayer electrode with the *anti*-DNP-Ab results in the electrochemical response shown in Figure 12 (curve d). Only a slight decrease in the electrocatalytic anodic current, as compared to the MRH^+-electrode itself, is observed. Thus, the *anti*-DNP-Ab does not associate to the MRH^+-monolayer electrode, and the electrical contact between Fc-GOx and the electrode is almost unaffected by the *anti*-DNP-Ab. These results clearly demonstrate that the dinitrospiropyran monolayer exhibits antigen affinity toward the *anti*-DNP-Ab, while the dinitromerocyanine monolayer, MRH^+-state, lacks affinity for the *anti*-DNP-Ab and does not act as an active antigen monolayer. Figure 12 (inset) shows the decrease in the amperometric responses of the dinitrospiropyran-antigen monolayer-electrode at different *anti*-DNP-Ab concentrations, using Fc-GOx and glucose as a redox probe to follow the formation

(46) The nitroaromatic functions of the dinitrospiropyran unit is electrochemically reduced to the Ar-NHOH derivative that yields a reversible redox-wave at 0.2 V vs SCE (Cf.: Tsutsumi, H.; Furumoto, S.; Morita, M.; Matsuda, Y. *J. Colloid Interfac. Sci.* **1995**, *171*, 505). This redox wave is used for the coulometric determination of the surface coverage of the photoisomerizable component. Nonetheless, these electrodes are discarded as the dinitrospiropyran units are irreversibly transformed to the Ar-NHOH and cannot be used for further analysis of the antigen−antibody interactions.

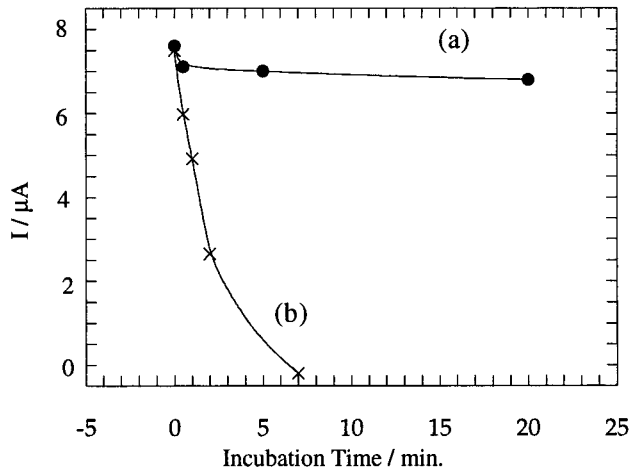

Figure 13. Amperometric responses of (a) **1a**-monolayer electrode and (b) **1b**-monolayer electrode upon interaction with the *anti*-DNP-Ab, 50 μg·mL^{-1} for different time intervals. Data were recorded at the same conditions as described in Figure 12 (inset).

of the antigen-antibody complex. The current responses decrease as the concentration of the *anti*-DNP-Ab increases, and ca. 85% of the characteristic amperometric signal of the redox probe are blocked at an *anti*-DNP-Ab concentration of 10 μg·mL^{-1} (incubation time: 6 min). The SP-monolayer electrode is thus an active antigenic interface for electrochemical detection of the *anti*-DNP-Ab in the concentration region of 0.5−5 μg·mL^{-1}.

The different affinities of the two photoisomer states of the monolayer-electrode for the *anti*-DNP-Ab are further reflected by following the rates of anti-DNP-Ab association to the photoisomerizable monolayer. Figure 13, curve a, shows the amperometric responses of the SP-monolayer electrode upon interaction with the *anti*-DNP-Ab solution (50 μg·mL^{-1}) for different time intervals, using Fc-GOx and glucose as a redox probe. The current responses of the electrode decrease as the time of incubation in the antibody solution is lengthened, and the amperometric signal is totally blocked after ca. 7 min of incubation in the *anti*-DNP-Ab solution (50 μg·mL^{-1}). Figure 13, curve b, shows the amperometric responses of the MRH$^+$-state monolayer electrode upon incubation at different time intervals with the *anti*-DNP-Ab solution (50 μg·mL^{-1}). The current responses are almost unaffected by the incubation time in the antibody solution. It is clear that the SP-monolayer exhibits antigen affinity toward the *anti*-DNP-Ab, while the MRH$^+$-state does not act as an active antigen monolayer for the anti-DNP-Ab. The different affinity features of the SP-monolayer, and the MRH$^+$-monolayer represents the prerequirement to tailor the reversible immunosensor devices.

To generate the reversible immunosensor electrode, the release of the *anti*-DNP-Ab bound to the SP-monolayer electrode must occur upon photoisomerization of the monolayer to the MRH$^+$-state. Figure 14 shows the cyclic amperometric responses of the monolayer electrode upon treatment with the *anti*-DNP-Ab, using Fc-GOx/glucose as redox probe. Interaction of the SP-monolayer electrode with the *anti*-DNP-Ab insulates the electrode toward the biocatalyzed oxidation of glucose as a result of the binding of the antibody to the antigen monolayer. Photoisomerization of the monolayer to the MRH$^+$-state followed by rinsing of the electrode surface regenerates the characteristic amperometric response of the MRH$^+$-monolayer electrode. This indicates that the *anti*-DNP-Ab was washed-off from the monolayer interface. Further photoisomerization of the MRH$^+$-monolayer electrode to the SP-monolayer state recycles the active antigen interface that is again insulated

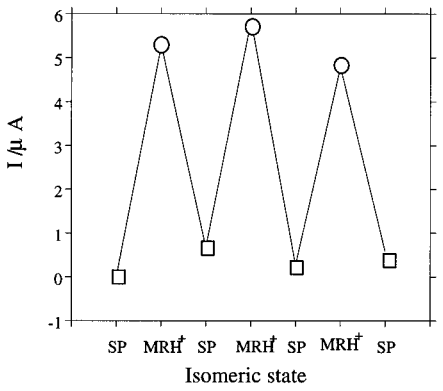

Figure 14. Cyclic amperometric responses of the dinitrospiropyran photoisomerizable monolayer electrode: (□) In the presence of the dinitrospiropyran monolayer-electrode, SP-state, after treatment with a *anti*-DNP-Ab solution (0.15 mg·mL^{-1}) for 6 min. (○) In the presence of the protonated dinitromerocyanine monolayer electrode MRH$^+$-state, produced by illumination of the *anti*-DNP-Ab associated with the SP-monolayer electrode followed by rinsing of the electrode with water. The SP-monolayer electrode was generated by irradiation of the MRH$^+$-monolayer electrode, λ > 495 nm. The MRH$^+$-monolayer electrode was produced by illumination of the *anti*-DNP-Ab − SP-monolayer electrode, 360 nm < λ < 380 nm. All measurements were performed in 0.01 M phosphate buffer, pH = 7.3, and sodium sulfate, 0.1 M, in the presence of Fc-GOx (5 mg·mL^{-1}) and glucose, 50 mM. Experiments were performed under Ar, 38 °C. Net electrocatalytic anodic currents at E = 0.4 V are presented.

upon interaction with the *anti*-DNP-Ab. Reversible photoisomerization of the SP-monolayer electrode with the bound *anti*-DNP-Ab to the MRH$^+$-monolayer state allows the washing-off of the associated Ab and by subsequent photoisomerization of the MRH$^+$-monolayer to the SP-state, the active sensing interface for the antibody is recycled.

The *anti*-DNP-Ab binding to the SP-monolayer and the dissociation from the MRH$^+$-monolayer interface was confirmed by QCM analyses. The photoisomerizable monolayer of the mercaptobutyl dinitrospiropyran, **1**, was assembled onto the Au-electrodes attached to the quartz crystal. The surface density of **1** was determined by following the frequency change after introducing the electrode into **1** solution (10 mM, DMF). A frequency change of $\Delta f = -150$ Hz was observed, indicating a surface coverage corresponding to ca. 2×10^{-9} mol·cm^{-2}. First, we followed the association of the *anti*-DNP-Ab both to the SP-monolayer and to MRH$^+$-monolayer-functionalized crystals. Figure 15, curves a and b, shows the frequency changes upon interaction of the SP-monolayer-functionalized crystal with two different concentrations of the *anti*-DNP-Ab. The decrease of the frequency indicates the association of the *anti*-DNP-ab to the SP-monolayer. The frequency change is higher as the antibody concentration increases: For the *anti*-DNP-Ab concentration of 30 μg·mL^{-1} the frequency change is $\Delta f = -120$ Hz (Figure 15, curve a), whereas for the lower antibody concentration (10 μg·mL^{-1}), the frequency decrease is only $\Delta f = -100$ Hz (Figure 15, curve b). Association of the *anti*-DNP-Ab to the antigen monolayer causes a mass increase at the electrode surface, and this is transduced by a decrease of the crystal resonance frequency. The same experiment was carried out for the MRH$^+$-monolayer-functionalized crystal, Figure 15, curves c and d. Only a slight decrease in the frequency is observed upon treatment of the MRH$^+$-monolayer with the *anti*-DNP-Ab. These results demonstrate again that the SP-monolayer exhibits antigen affinity toward the *anti*-DNP-Ab, whereas the MRH$^+$-monolayer lacks affinity for the *anti*-DNP-Ab and does not act as an active antigen interface.

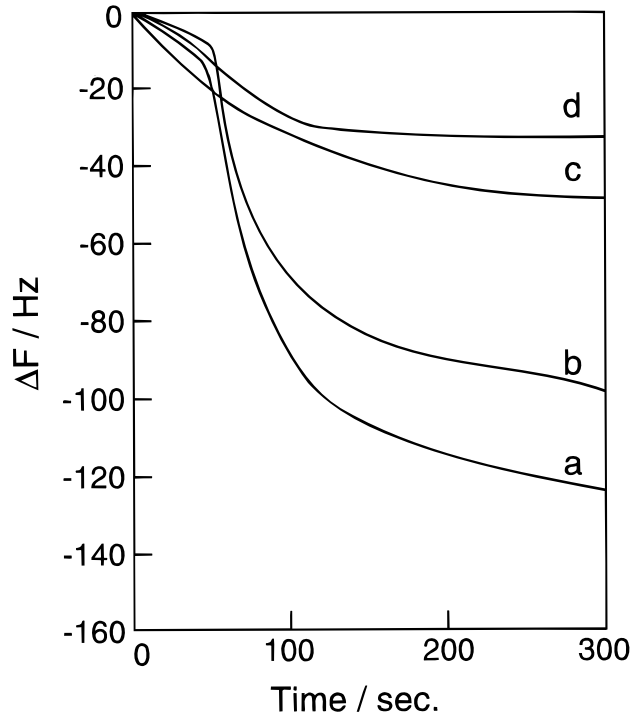

Figure 15. Time-dependent frequency changes of a **1**-monolayer assembled onto a Au-quartz crystal: (a) and (b) in the presence of the **1a**-monolayer electrode and *anti*-DNP-Ab, 30 μg·mL^{-1} 10 μg·mL^{-1}, respectively; (c) and (d) in the presence of **1b**-monolayer electrode in the presence of the *anti*-DNP-Ab, 30 μg·mL^{-1} and 10 μg·mL^{-1}, respectively.

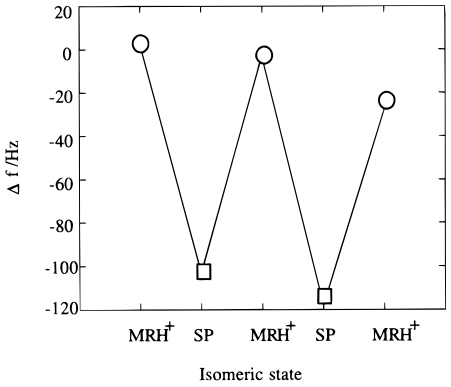

Figure 16. Cyclic microgravimetric QCM analysis of the association and dissociation of anti-DNP-Ab to and from the photoisomerizable monolayer interface. (○) Frequency of the protonated dinitromerocyanine monolayer-modified quartz crystal, MRH$^+$-state. (□) Frequency of the dinitrospiropyran monolayer-modified crystal, SP-state, after treatment with anti-DNP-Ab (10 μg·mL^{-1}). The SP-monolayer associated with the quartz crystal was generated by irradiation of the MRH$^+$-monolayer, $\lambda > 495$ nm. The MRH$^+$-monolayer on the quartz crystal was generated by irradiation of the bare SP-monolayer electrode (first cycle) or of the SP-monolayer electrode with associated anti-DNP-Ab (any other cycle), 360 nm $< \lambda <$ 380 nm, followed by rinsing with water. All measurements were recorded in PBS buffer at 25 °C. The frequency changes of the crystal as a result of the association of anti-DNP-Ab to the SP-monolayer electrode stabilized to a constant value after ca. 5 min. Dissociation of the anti-DNP-Ab from the MRH$^+$-monolayer state was performed outside of the cell via U.V.-irradiation (3 min) followed by rinsing (30 s). The presented frequency value represents the crystal frequency after mounting the crystal in the cell and stabilization to constant frequency (ca. 10 min).

Figure 16 shows the frequency changes of the modified quartz-crystal in the two photoisomer states of the monolayer upon interaction with the *anti*-DNP-Ab. Treatment of the SP-monolayer-modified crystal results in a frequency change corresponding to $\Delta f = -105$ Hz. The frequency decrease indicates that upon interaction of the crystal with the *anti*-DNP-Ab, the crystal mass increased by ca. $\Delta m = 574$ ng·cm^{-2}. This originates from the association of the *anti*-DNP-Ab to the antigen monolayer interface. From the observed frequency change (Δf), we estimate the surface coverage of the *anti*-DNP-Ab on the Au-surface associated with the crystal to be 3.83×10^{-12} mol·cm^{-2}. Photoisomerization of the monolayer associated with the crystal to the MRH$^+$-state, followed by rinsing of the crystal, results in the original base-frequency of the monolayer-modified crystal, prior to treatment with the *anti*-DNP-Ab. Control experiments revealed that no noticeable frequency changes of the monolayer-modified crystal occur upon photoisomerization of the SP-monolayer to the MRH$^+$-monolayer state. The results described in Figure 16, where the base frequency of the crystal is observed in the presence of the MRH$^+$-monolayer and the *anti*-DNP-Ab, differ slightly from the time-dependent frequency changes of the MRH$^+$-monolayer crystal addressed in Figure 15. In Figure 15 we see a slight time-dependent frequency decrease, implying the association of the *anti*-DNP-Ab to the interface, whereas in Figure 16 the crystal does not show a frequency alteration upon treatment of the crystal with the *anti*-DNP-Ab. This apparent inconsistency originates from the fact that the *anti*-DNP-Ab is nonspecifically adsorbed to the MRH$^+$-monolayer-functionalized crystal, a property that is reflected in Figure 16. In the experimental results shown in Figure 16, the MRH$^+$-generated monolayer is rinsed prior to the recording of the crystal frequency. This results in the dissociation of the nonspecific adsorbates and the observation of the base frequency of the monolayer-modified-crystal. Thus, the recovery of the base frequency of the quartz-crystal upon photoisomerization of the SP-monolayer-modified surface with bound *anti*-DNP-Ab to the MRH$^+$-state is attributed to the dissociation of the Ab from the interface. By subsequent isomerization of the MRH$^+$-monolayer-modified crystal to the SP-state followed by interaction with the DNP-Ab, the characteristic decrease in the crystal frequency is observed, implying that association of the antibody to the surface reoccurred. The electrochemical and QCM experiments reveal that the dinitrospiropyran photoisomerizable antigen monolayer electrode can be used as a reusable sensing interface for the *anti*-DNP-Ab. The QCM experiments indicate that *anti*-DNP-Ab is associated to the SP-monolayer state and is dissociated from the monolayer upon photoisomerization of the monolayer to the MRH$^+$-state. The possibility to bind the *anti*-DNP-Ab to the monolayer that was photoisomerized from the MRH$^+$-state to the SP-state implies that the active antigen monolayer was regenerated. The QCM microgravimetric analysis of the association and dissociation of the *anti*-DNP-Ab to and from the photoisomer states of the monolayer correlates nicely with the amperometric responses of the electrode in the presence of Fc-GOx and glucose as redox probe. Association of the *anti*-DNP-Ab to the SP-monolayer electrode blocks the electrical contact between Fc-GOx, and the electrode, and the bioelectrocatalyzed oxidation of glucose is inhibited. Photoisomerization of the monolayer consisting of the antigen−antibody complex to the MRH$^+$-state results in the dissociation of the Ab from the monolayer interface. This is reflected by the high amperometric response of the electrode as well as by the decrease in the electrode mass in the QCM experiments. By further isomerization of the MRH$^+$-monolayer electrode to the SP-state, the active sensing interface is regenerated. It should be noted that rinsing of the electrodes upon photoisomerization of the monolayer to the MRH$^+$-state is essential to induce the dissociation of the *anti*-DNP-Ab. This

could originate from nonspecific adsorption of the Ab to the monolayer interface that is easily removed by the rinsing process. The reversible association/dissociation of the *anti*-DNP-Ab from the photoisomerizable monolayer was cycled ten times with no noticeable deterioration of the electrode surface.

Conclusions

The present study addressed basic configurations for electrochemical and microgravimetric, quartz-crystal-microbalance, sensing of antibodies or antigens. One concept is based on the assembly of an antigen monolayer on a Au-electrode and the electrode insulation toward a redox-probe in solution by the association of the complementary antibody to the monolayer interface. The second concept is based on the organization of an antigen monolayer on a quartz crystal and the microgravimetric sensing of mass changes at the antigen monolayer as a result of the antibody association. The electrochemical method was successfully applied to sense the *anti*-DNP-Ab (or the Nϵ-2,4-dinitrophenyllysine, **3**, antigen) by means of a dinitrophenyllysine monolayer-functionalized-electrode, using the $Fe(CN)_6^{3-}/Fe(CN)_6^{4-}$ as a redox probe. An "electrically-wired" redox enzyme, glucose oxidase, modified by ferrocene units, Fc-GOx, was found to be a superior redox-probe to follow the antibody−antigen complex at the electrode interface. The latter macromolecular redox-probe is insensitive to molecular defects or "pinholes" in the monolayer composition and enables the bioelectrocatalytic amplification of the antigen−Ab complex formation at the monolayer-electrode. This antigen-monolayer-electrode configuration can be further modified to other electrochemical immunosensing electrodes. Also, the concept of electrode insulation by biospecific interactions at a monolayer-functionalized electrode could be applied to develop sensing interfaces for other biorecognition pairs. The piezoelectrical, microgravimetric, method to sense an antibody or an antigen was exemplified with the organization of the 3,5-dinitrosalicylic acid antigen monolayer on Au-electrodes associated with a quartz crystal. *anti*-DNP-Ab or 2,4-dinitrophenol was analyzed by this monolayer interface using the microgravimetric method.

Another important aspect of the present study is the demonstration that biospecific antigen−antibody interactions can be photostimulated by the application of photoisomerizable antigens. Specifically, we addressed the light-induced association and dissociation of the *anti*-DNP-Ab to the photoisomerizable dinitrospiropyran monolayer. The photochemically triggered association and dissociation of antigen−antibody complexes on solid supports represents a major advance in immunosensor technology as it reveals a novel method to tailor reversible, reusable immunosensors. Other potential applications of photostimulated antigen−antibody affinity interactions include antibody patterning on photolithographically patterned photoisomerizable antigen layers, microstructuring of biomaterials on surfaces via deposition of antibody-biomaterial conjugates onto photoisomerizable antigen interfaces, and tailoring of rechargeable biomaterial layers, i.e., enzymes, via coupling of photoisomerizable antigen-modified biomaterials to antibody-functionalized supports and the application of photostimulated antigen−antibody interactions in the assembly of optobioelectronic devices. Preliminary studies indeed revealed the possibility to pattern the dinitrospiropyran photoisomerizable antigen monolayers with the *anti*-DNP-Ab[47] and to couple the DNP-Ab to a dinitrospiropyran-modified redox-enzyme to yield a biphasic optobioelectronic switch for amperometric transduction of recorded optical signals.[48]

Acknowledgment. The support of this study by the Bundesministerium für Bildung, Wissenschaft, Forschung und Technologie, BMBF, Germany, and the Israel Ministry of Science, MOS, is gratefully acknowledged.

Supporting Information Available: The calibration curve corresponding to the amperometric responses of **3**-modified monolayer electrode in the presence of different concentrations of *anti*-DNP-Ab and using $K_3Fe(CN)_6$ as redox probe (2 pages). See any current masthead paper for ordering and Internet access information.

JA971980Z

(47) Willner, I.; Blonder, R. *Thin Solid Films* **1995**, *266*, 254.
(48) Lion-Dagan, M.; Katz, E.; Willner, I. *J. Am. Chem. Soc.* **1994**, *116*, 7913.